# Cytotoxic T-lymphocyte-associated protein 4-Ig effectively controls immune activation and inflammatory disease in a novel murine model of leaky severe combined immunodeficiency

Stéphanie Humblet-Baron, MD, PhD,[a,b] Susann Schönefeldt, MSc,[a,b] Josselyn E. Garcia-Perez, MSc,[a,b] Frédéric Baron, MD, PhD,[c] Emanuela Pasciuto, PhD,[a,b] and Adrian Liston, PhD[a,b] *Leuven and Liege, Belgium*

**Background: Severe combined immunodeficiency can be caused by loss-of-function mutations in genes involved in the DNA recombination machinery, such as recombination-activating gene 1 *(RAG1)*, *RAG2*, or DNA cross-link repair 1C *(DCLRE1C)*. Defective DNA recombination causes a developmental block in T and B cells, resulting in high susceptibility to infections. Hypomorphic mutations in the same genes can also give rise to a partial loss of T cells in a spectrum including leaky severe combined immunodeficiency (LS) and Omenn syndrome (OS). These patients not only experience life-threatening infections because of immunodeficiency but also experience inflammatory/autoimmune conditions caused by the presence of autoreactive T cells.**

**Objective: We sought to develop a preclinical model that fully recapitulates the symptoms of patients with LS/OS, including a model for testing therapeutic intervention.**

**Methods: We generated a novel mutant mouse *(Dclre1c$^{leaky}$)* that develops a LS phenotype. Mice were monitored for diseases, and immune phenotype and immune function were evaluated by using flow cytometry, ELISA, and histology.**

**Results: *Dclre1c$^{leaky}$* mice present with a complete blockade of B-cell differentiation, with a leaky block in T-cell differentiation resulting in an oligoclonal T-cell receptor repertoire and enhanced cytokine secretion. *Dclre1c$^{leaky}$* mice also had inflammatory symptoms, including wasting, dermatitis, colitis, hypereosinophilia, and high IgE levels. Development of a preclinical murine model for LS allowed testing of potential treatment, with administration of cytotoxic T-lymphocyte-associated protein 4-Ig reducing disease symptoms and immunologic disturbance, resulting in increased survival.**

**Conclusion: These data suggest that cytotoxic T-lymphocyte-associated protein 4-Ig should be evaluated as a potential treatment of inflammatory symptoms in patients with LS and those with OS. (J Allergy Clin Immunol 2017;■■■:■■■-■■■.)**

*Key words: Leaky severe combined immunodeficiency, Artemis, regulatory T cell, cytotoxic T-lymphocyte-associated protein 4, immune dysregulation*

Severe combined immunodeficiency (SCID) disorders are characterized by a profound defect in the adaptive immune system with a partial or total loss of function of T and B cells. Patients are highly susceptible to severe opportunistic infections, and their survival expectancy is limited unless they receive early allogeneic hematopoietic stem cell transplantation. An important cause of SCID is mutation in genes, such as recombination-activating gene 1 *(RAG1)*, *RAG2*, DNA cross-link repair 1C *(DCLRE1C)*, and DNA ligase 4 *(LIG4)*, which produce proteins that are part of the DNA recombination machinery. During the V(D)J recombination of the T-cell receptor (TCR) or B-cell receptor (BCR), RAG1 and RAG2 recognize the recombination signal sequence and cleave double-stranded DNA, followed by formation of the hairpin loop at the end of the open DNA. In complex with other proteins, ARTEMIS (the product of *DCLRE1C*) then cleaves these hairpin loops to allow ligation of the newly formed DNA strand by DNA ligase IV (the product of *LIG4*). In the absence of any of these components, defective V(D)J recombination blocks the formation of a functional TCR or BCR, leading to an early block of T- and B-cell differentiation.[1]

In addition to the typical SCID phenotype, hypomorphic mutations in the *RAG1*, *RAG2*, and *DCLRE1C* genes can cause Omenn syndrome (OS) and leaky severe combined immunodeficiency (LS). OS is characterized by early and severe inflammatory symptoms, including generalized erythroderma, diarrhea, hepatosplenomegaly, lymphadenopathy with hypereosinophilia, and increased IgE levels. Unlike SCID, T cells are detected in the blood of patients in the absence of maternal engraftment and demonstrate peripheral activation and oligoclonal expansion of self-reactive T cells.[2] Patients with LS show even higher levels of blood T cells (although still reduced relative to those in healthy subjects) of an oligoclonal nature.[2] Patients with LS can present with a later clinical onset of disease with combined immunodeficiency and immune dysregulation, leading to autoimmune manifestations, mostly autoimmune cytopenia. Both patients with OS and those with LS are highly susceptible to cancer of lymphoid origin.[3] In most patients with OS and LS, residual activity of the protein is detected. Specifically, large deletions and mutations in the catalytically functional domains (β-lactamase and β-CASP

From [a]VIB Center for Brain & Disease Research, Leuven; [b]KU Leuven, Department of Microbiology and Immunology, Leuven; and [c]GIGA I[3] and Department of Hematology, University of Liege.

Supported by the Jeffrey Modell Foundation (Gene therapy for IPEX), FWO (1272517N), and IUAP (T-TIME). S.H.-B. was supported by an FWO postdoctoral fellowship.

Disclosure of potential conflict of interest: S. Humblet-Baron has received grants from FWO. F. Baron has received travel support from Celgene, Sanofi, Amgen, Pfizer, and Roche. A. Liston has received grants from FWO, IUAP, and the Jeffrey Modell Foundation. The rest of the authors declare that they have no relevant conflicts of interest.

Received for publication June 15, 2016; revised November 6, 2016; accepted for publication December 1, 2016.

Corresponding author: Adrian Liston, PhD, Department of Microbiology and Immunology, University of Leuven, Herestraat 49, bus 1026, 3000 LEUVEN, Belgium. E-mail: adrian.liston@vib.be.

0091-6749/$36.00



http://dx.doi.org/10.1016/j.jaci.2016.12.968

*Abbreviations used*

BCR: B-cell receptor
CTLA4: Cytotoxic T-lymphocyte-associated protein 4
DCLRE1C: DNA cross-link repair 1C
ENU: *N*-ethyl-*N*-nitrosourea
Foxp3: Forkhead box p3
GFP: Green fluorescent protein
LIG4: DNA ligase 4
LS: Leaky severe combined immunodeficiency
OS: Omenn Syndrome
RAG: Recombination-activating gene
SCID: Severe combined immunodeficiency
SP: Single-positive
TCM: Central memory T
TCR: T-cell receptor
Treg: regulatory T

domains) of the ARTEMIS protein lead to an absence of protein and SCID, whereas mutations in the C-terminal domain can result in OS/LS phenotypes.[4] OS and LS appear to lie on a spectrum of immunodeficiency, with potential for similar mutations to manifest with different clinical presentations.[3,5]

A diverse set of hypotheses have been formulated to explain the coexistence of autoimmunity and immunodeficiency in patients with OS/LS.[6] However, the lack of preclinical models for LS/OS with ARTEMIS deficiency has restricted both a functional understanding of the immune processes occurring and also the testing of therapeutic tools. Here we developed a novel LS mouse model caused by a hypomorphic point mutation in *Dclre1c*. Mutant mice have a macroscopic phenotype similar to that of patients with LS, including the presence of peripheral T-cell lymphocytes, development of spontaneous inflammatory diseases, and a high incidence of lymphoma development. Importantly, administration of the immunosuppressive drug cytotoxic T-lymphocyte-associated protein 4-Ig (CTLA4-Ig) resulted in control of inflammation and improved disease-free survival in comparison with control mice, identifying CTLA4-Ig as a potential treatment for patients with LS.

# METHODS

## Mice

Founder C57BL/6 male mice were treated with 100 mg/kg *N*-ethyl-*N*-nitrosourea (ENU) and bred to *Foxp3*$^{GFP}$ female mice to generate the *Dclre1c*$^{leaky}$ strain.[7] First-generation male offspring were backcrossed to *Foxp3*$^{GFP}$ female mice to produce second-generation offspring, which were in turn intercrossed to produce the third generation for phenotype screening. Phenotype screening involved flow cytometric analysis for CD4 and Foxp3 (GFP) and identification of mice with values for the percentage of GFP$^+$ cells (within the CD4$^+$ population) more than 2 SDs from the norm. Identified variant offspring were intercrossed to produce the C57BL/6.*Foxp3*$^{GFP}$.*Dclre1c*$^{leaky}$ mutant mouse strain. The *leaky* mutation was identified by means of all-exome sequencing and confirmed by using Sanger sequencing.

CTLA4-Ig (abatacept [Orencia]; Bristol-Myers Squibb, New York, NY) was administrated to C57BL/6.*Foxp3*$^{GFP}$.*Dclre1c*$^{leaky}$ and littermate control mice starting at 8 weeks of age at a dose of 25 mg/kg administered intraperitoneally every other week. Mice were maintained in specific pathogen-free facilities of the University of Leuven. All experiments were approved by the University of Leuven ethics committee.

## Western blotting

Thymocytes were homogenized in lysis buffer consisting of 100 mmol/L NaCl, 50 mmol/L Tris-HCl (pH 7.5), 1% Triton X-100, 2 mmol/L dithiothreitol, 1 mmol/L EDTA, phosphatase inhibitor (Sigma-Aldrich, St Louis, Mo), and protease inhibitor (Pierce, Rockford, Ill) and then incubated on ice for 30 minutes. Cells were sonicated, and lysate was prepared. The NuPAGE Precast Gel System was used for Western blotting (Life technologies, Grand Island, NY). Ten to 20 μg of lysate was separated on 4-12% bis-Tris acrylamide gels and blotted on a polyvinylidene difluoride membrane (GE Healthcare, Fairfield, Conn). Membranes were incubated with polyclonal IgG rabbit anti-mouse/human Artemis (1:1000, PA5-26741; Thermo Scientific, Waltham, Mass) and mouse anti–glyceraldehyde-3-phosphate dehydrogenase (GAPDH; 1:10000, GA1R; Thermo Scientific) and developed by using Western Lightning Plus-ECL (PerkinElmer, Waltham, Mass) and the imaging system G:Box XRQ (Syngene, Cambridge, United Kingdom). Quantification was performed with AIDA software (version 5.0; Raytest, Straubenhardt, Germany).

## TCR Vβ CDR3 size spectratype analysis

Total splenocytes were harvested and conserved in RNA Later stabilization reagent (Trizol, Thermo Fisher Scientific). RNA was then extracted with the RNEasy Mini Kit (Qiagen, Hilden, Germany), according to the manufacturer's instructions. Genomic DNA was removed by using recombinant RNase-free DNaseI (Roche, Mannheim, Germany). cDNA was synthesized from RNA (2 μg) by using oligo(dT)$_{18}$ primers with the Transcriptor First Strand cDNA Synthesis Kit (Roche). Seminested PCR was performed with sense primers for a panel of murine Vβ families and 2 Cβ anti-sense primers (Integrated DNA Technologies, Leuven, Belgium), as previously described. CDR3 size spectratype analysis was performed with GeneMapper version 4.0 Software (Applied Biosystems, Foster City, Calif).

## Flow cytometry

Single-cell suspensions were prepared from mouse thymus, bone marrow, spleen, and pooled lymph nodes (cervical, inguinal, mesenteric, axillary, and brachial). For intracellular cytokine staining, lymphocytes were plated at $5 \times 10^5$ cells/well in 96-well tissue-culture plates in complete RPMI containing phorbol 12-myristate 13-acetate (50 ng/mL; Sigma-Aldrich), ionomycin (250 ng/mL; Sigma-Aldrich), and monensin (1/1500; BD Biosciences, San Jose, Calif) for 4 hours at 37°C. All cells were fixed with BD Cytofix (BD Biosciences) or fixed and permeabilized with the eBioscience Foxp3 staining kit (eBioscience/Affymetrix, San Diego, Calif). Anti-murine antibodies included anti-CD4 (RM4-5), anti-CD8α (53-6.7), anti-Foxp3 (FJK-16s), anti-CD25 (PC61.5), anti-CTLA4 (UC10-4B9), anti-CD69 (H1.2F3), anti-CD44 (IM7), anti–CD62 ligand (MEL-14), anti-B220 (RA3-6B2), anti-CD19 (eBio1D3), anti-CD43 (eBioR2/60), anti-IgM (II/41), anti-IgD (11-26c), anti-NK1.1 (PK136), anti-Gr1 (RB6-8C5), anti-CD11b (M1/70), anti-CD127 (A7R34), anti-KLRG1 (2F1), anti-PD1 (J43), anti-CD3 (145-2c11), anti-CD24 (M1/69), anti-Qa2 (1-1-2), anti-NKG2D (CX5), anti-Ly49D (4E5), anti-CD122 (TM-b1), anti–IFN-γ (XMG1.2), anti–IL-4 (BVD6-24G2), and anti–IL-17 (eBio17B7) from eBioscience and anti-Ki67 (B56) and anti–Siglec-F (E50-2440) from BD Biosciences.

## Histology

Mouse tissues were preserved in 10% formalin and processed into paraffin-embedded tissue blocks by Histology Consultation Services (Everson, Wash). Each block had thin (approximately 4-μm) sections cut on a microtome, mounted on glass slides, and stained with hematoxylin and eosin. Pathological diagnosis was performed by Biogenetics Research Laboratories, Greenbank, Wash.

## ELISA-MSD

IgE titers in individual serum samples were determined by using a mouse IgE ELISA Ready-SET-Go! Kit (eBioscience), according to the manufacturer's protocol. Cytokine serum levels were quantified by using V-Plex mouse Pro-inflammatory panel MSD (Meso Scale Discovery, Rockville, Md) plates, according to the manufacturer's instructions.

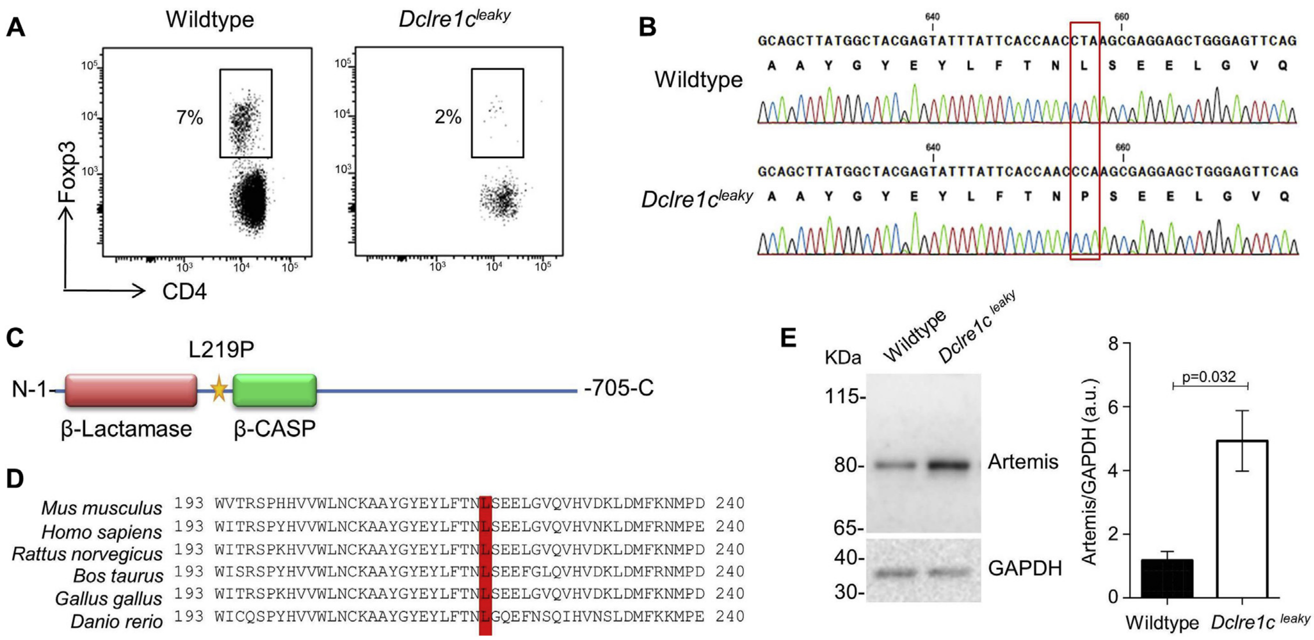


**FIG 1.** New point mutation identified in *Dclre1c$^{leaky}$* mice. By using ENU mutagenesis, *leaky* mice with a point mutation in ARTEMIS were identified. **A,** *Leaky* mice were identified with a low level of peripheral Treg cells in the blood. **B,** Sanger sequencing of *Dclre1c*, encoding for ARTEMIS, in wild-type and *leaky* mice confirmed a T-to-C mutation resulting in a lysine-to-proline mutation in amino acid change. **C,** Mutation confers a L219P substitution *(star)* between the 2 active domains of the protein (β-lactamase, SM00849, and the β-CASP domain PF07522). **D,** L219P mutation is located in a region conserved across species. **E,** Western blot *(left)* and relative expression *(right)* of ARTEMIS protein in thymocytes from wild-type (n = 5) and *Dclre1c$^{leaky}$* (n = 5) mice. *GAPDH*, Glyceraldehyde-3-phosphate dehydrogenase.

## Statistical analyses

Single comparisons were analyzed by using the nonparametric Mann-Whitney *U* test. All statistical analyses were carried out with GraphPad Prism (GraphPad Software, La Jolla, Calif). Data from mice diagnosed with tumors were excluded from cell subset and cytokine analysis. Homology alignment was performed by using HomoloGene and BLAST.

## RESULTS

### An ENU-induced mutation in ARTEMIS results in an LS phenotype

In a screen for modulators of regulatory T (Treg) cell numbers, we exposed C57Bl/6 mice to the ENU mutagen and intercrossed with the *Foxp3$^{GFP}$* strain before flow cytometry–based screening for Treg cell numbers. One pedigree was isolated with the presentation of low CD4$^+$ T-cell counts and disproportionately low Treg cell counts within the blood (Fig 1, *A*). All-exon sequencing identified a point mutation in *Dclre1c*, the gene encoding ARTEMIS. This transition mutation (c.656T>C), named *leaky*, generated an amino acid substitution in position 219 coding for a proline instead of a leucine (Fig 1, *B*). The mutated residue is located between the β-lactamase and β-CASP domains in a highly conserved region (Fig 1, *C* and *D*). Western blot analysis detected a strong presence of ARTEMIS expression in the *leaky* mouse thymus, indicating that the mutation did not affect protein expression (Fig 1, *E*).

The discrepancy between *Dclre1c$^{KO}$* mice,[8] with near-complete T cell deficiency, and *Dclre1c$^{leaky}$* mice, with reduced but detectable numbers of T cells in all mice, spurred further characterization of T-cell development in the mutant strain. *Dclre1c$^{KO}$* mice display a block in thymocyte development at the double-negative stage during VDJ rearrangement.[8] *Dclre1c$^{leaky}$* mice also exhibited decreased absolute numbers of total thymic cells in comparison with wild-type mice (Fig 2, *A*). Furthermore, percentages of double-negative cells were enhanced in ARTEMIS mutant mice compared with those in wild-type mice in both young and old animals (Fig 2, *B*). Double-positive cell counts were severely reduced in *leaky* mice (Fig 2, *C*); however, unlike knockout animals, both single-positive (SP) CD8$^+$ T cells (SP CD8$^+$) and CD4$^+$ T cells (SP CD4$^+$) were detected in *Dclre1c$^{leaky}$* mice (Fig 2, *D* and *E*). This result indicates a hypomorphic allele, allowing a fraction of thymocytes to rearrange competent TCRs for further progress to the next developmental stage. Detailed immunophenotyping of the thymus showed a dominant presence of recirculating cells within the SP T-cell population in *Dclre1c$^{leaky}$* mice in comparison with wild-type animals (see Fig E1 in this article's Online Repository at www.jacionline.org). Interestingly and in line with the initial phenotype screening, Foxp3$^+$ Treg cell counts were significantly decreased in both young and old mutant animals (Fig 2, *F*). In absolute numbers all measured T-cell subsets in the thymus were decreased in *leaky* mice, but substantial numbers of T cells were still able to rearrange their TCR and mature to the periphery (see Fig E1).

The LS phenotype in human subjects has been described as a strongly reduced but still present number of CD3$^+$ T cells in the peripheral blood caused by hypomorphic mutation in known SCID genes, including *DCLRE1C*.[2] In *Dclre1c$^{leaky}$* mice both mature CD4$^+$ and CD8$^+$ T cells were present in the spleen, although at significantly lower numbers (Fig 3, *A-C*, and see Fig E2, *D*, in this article's Online Repository at www.jacionline.org).

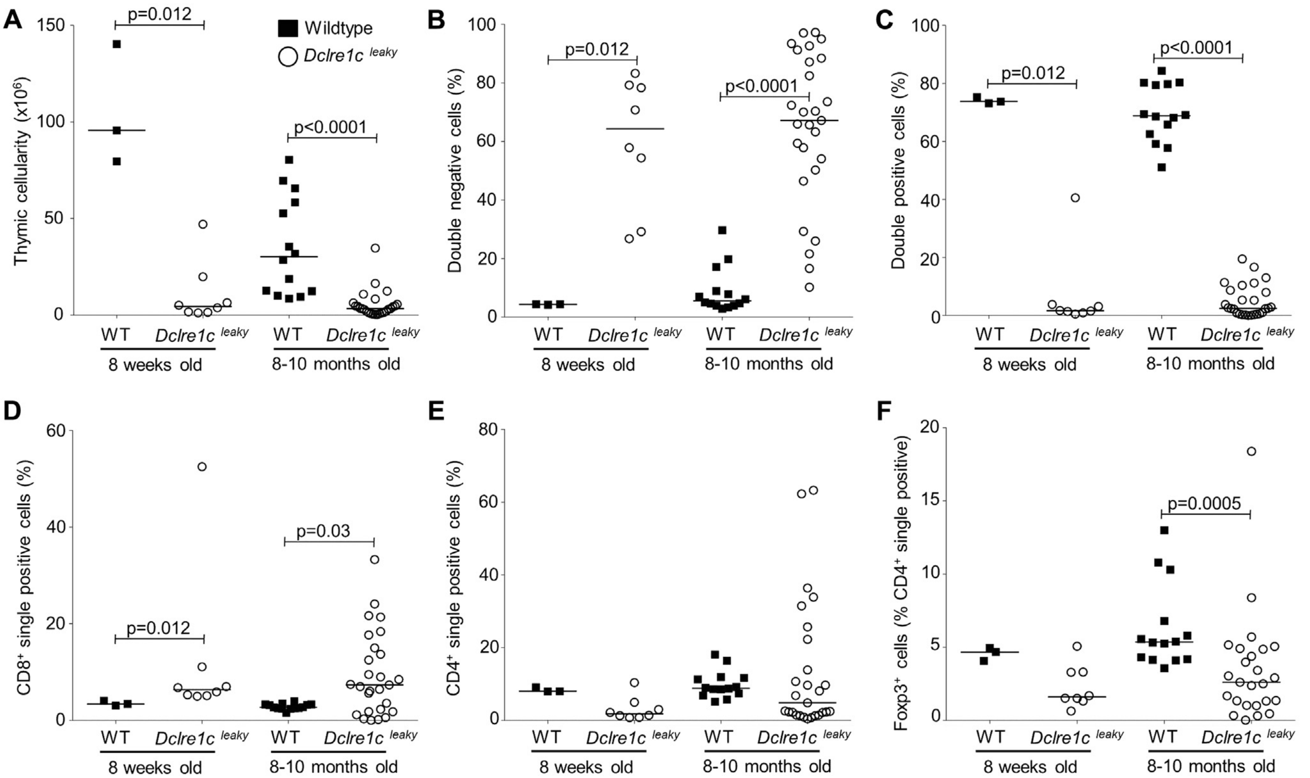


**FIG 2.** Partial T-cell developmental block in *Dclre1c$^{leaky}$* mice. The thymi of wild-type *(WT)* and *Dclre1c$^{leaky}$* mice were evaluated at 8 weeks and 8 to 10 months of age. Thymic cell subsets were analyzed by using flow cytometry. **A,** Thymus absolute cell numbers. **B,** Percentage of double-negative cells from total cells. **C,** Percentage of double-positive cells from total cells. **D,** Percentage of CD8$^+$ single-positive cells from total cells. **E,** Percentage of CD4$^+$ single-positive cells from total cells. **F,** Percentage of Treg cells from single-positive CD4$^+$ cells. Median and individual data points are shown. Pooled data from up to 11 experiments are shown: wild-type 8-week-old mice (n = 3), *Dclre1c$^{leaky}$* 8-week-old mice (n = 8), wild-type 8- to 10-month-old mice (n = 14), and *Dclre1c$^{leaky}$* 8- to 10-month-old mice (n = 27).

T cells were also present in the lymph nodes (see Fig E2). Importantly, in almost all *leaky* mice analyzed, Treg cell numbers were disproportionately reduced (Fig 3, *D*, and see Fig E2, *E*). Patients with an LS phenotype have a restricted T-cell repertoire.[2] This prompted us to analyze the diversity of the TCR repertoire in the spleens of wild-type and *leaky* mice through TCR spectratyping. Consistent with the patient phenotype, we observed that *Dclre1c$^{leaky}$* mice displayed a very limited TCR repertoire compared with wild-type mice (Fig 3, *E*). Together, these results indicate that *leaky* mice recapitulate the oligoclonal nature of the T-cell repertoire observed in patients with LS because of restricted T-cell differentiation.

Regarding other immune cell compartments, B cells were almost absent in *leaky* mice, with an early block between the pro–B-cell and pre–B-cell stage during bone marrow development with a conserved pro–B-cell compartment (median, 3.3% from total bone marrow cells for wild-type mice vs 3.4% for *Dclre1c$^{leaky}$* mice) and a near-absent pre–B-cell compartment (median, 4.3% from total bone marrow cells for wild-type mice vs 0.2% for *Dclre1c$^{leaky}$* mice; $P$ = .003; Fig 3, *F* and *G*). The percentage of natural killer and myeloid cells was increased in ARTEMIS mutant mice because of the reduction in T- and B-lymphocyte numbers, but absolute numbers were similar (Fig 3, *H-J*). However, an altered activation profile was observed in natural killer cells from *Dclre1c$^{leaky}$* mice (see Fig E2, *F* and *G*). Therefore *Dclre1c$^{leaky}$* mice fit the immunologic criteria for LS, with severe but partial defects in TCR/BCR rearrangement but otherwise intact immune systems.

## *Leaky* mice develop inflammatory pathology

Published mice with mutations in ARTEMIS phenocopy the classical SCID presentation of patients with *DCLRE1C* mutations,[8-11] with defects in T and B cells causing immunodeficiency but no spontaneous disease,[8-11] apart from an increased incidence of tumor under a specific backcross.[12] By contrast, *Dclre1c$^{leaky}$* mice recapitulate the LS phenotype present in a subset of *DCLRE1C* patients[13] with spontaneous immune activation. The clonal T cells from *leaky* mice that underwent successful TCR rearrangement demonstrated high levels of oligoclonal peripheral expansion (Fig 3, *E*), with enhanced proliferation (Fig 4, *A*, and see Fig E3, *A*, in this article's Online Repository at www.jacionline.org). These expanded cells were mainly of an effector phenotype, with a significantly decreased naive T-cell compartment (Fig 4, *B* and *C*, and Fig E3, *B* and *C*). Interestingly, CD122 expression was increased in CD8$^+$ central memory T (TCM) cells, suggesting that *Dclre1c$^{leaky}$* T cells might have a higher reliance on IL-15 for homeostasis (see Fig E3, *D*). This is further illustrated by an expansion over time of this specific CD8$^+$ TCM cell population in *Dclre1c$^{leaky}$* mice, whereas this

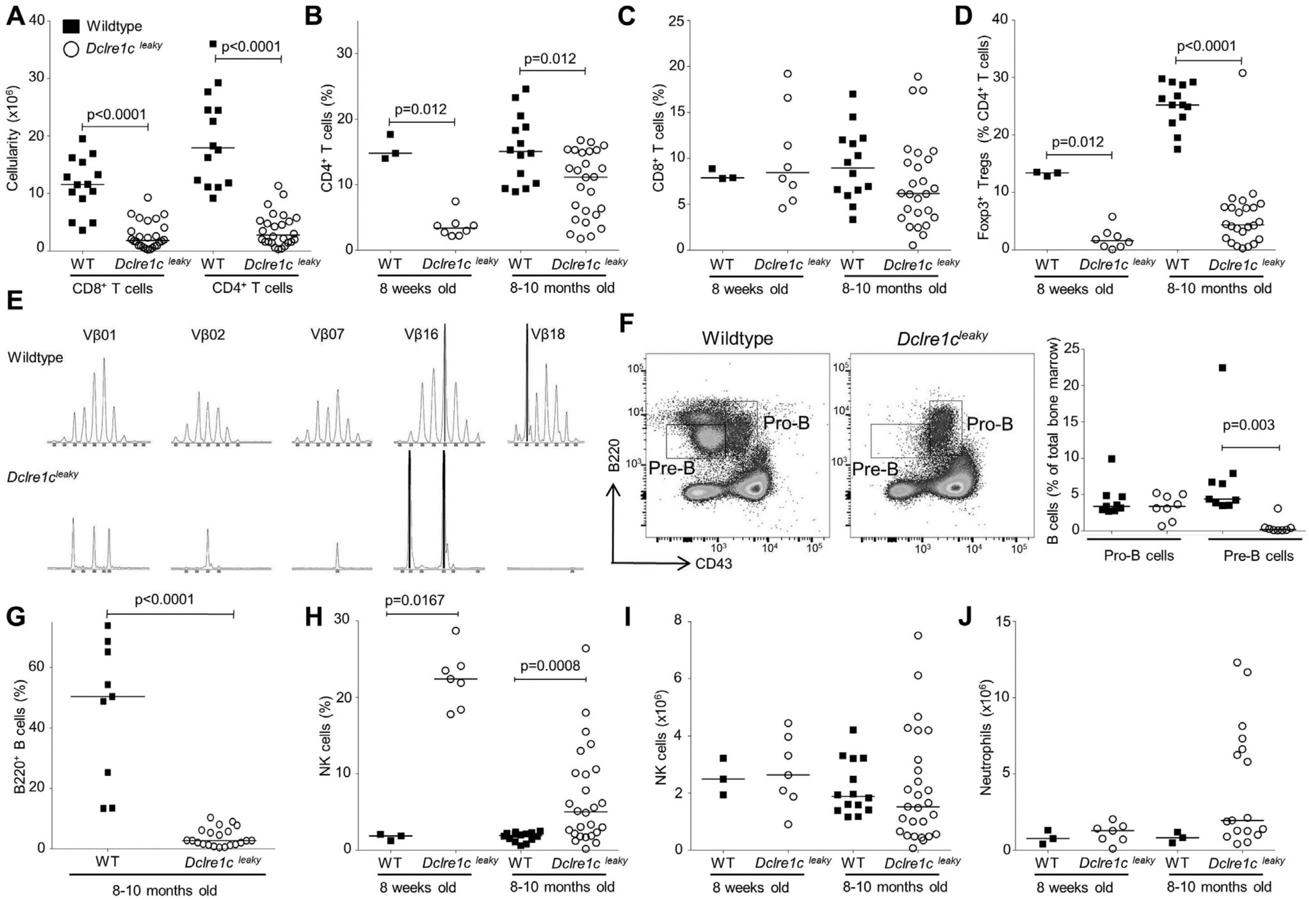


**FIG 3.** *Dclre1c$^{leaky}$* mice have an LS phenotype in the periphery. Spleens from wild-type *(WT)* and *Dclre1c$^{leaky}$* mice were evaluated at 8 weeks and between 8 and 10 months of age. Splenic cell subsets were analyzed by using flow cytometry. **A,** Absolute numbers of CD8$^+$ and CD4$^+$ T cells in the spleen at 8 to 10 months. **B-D,** Percentage of CD4$^+$ T cells (Fig 3, *B*), CD8$^+$ T cells (Fig 3, *C*), and Treg cells (CD4$^+$Foxp3$^+$ cells; Fig 3, *D*). **E,** Spectratyping CDR3 analysis of TCR Vβ diversity. Representative mice and Vβ families are presented. *Black bars* indicate saturation of signal intensity. **F,** Representative bone marrow B-cell maturation flow cytometric plots *(left)* and percentage of early B-cell progenitors (pro–B cells and pre–B cells graph; *right*). **G** and **H,** Percentage of splenic B cells (Fig 3, *G*) and natural killer cells (Fig 3, *H*). **I** and **J,** Absolute numbers of splenic natural killer cells (Fig 3, *I*) and neutrophils (Gr-1$^{high}$/CD11b$^{high}$ cells; Fig 3, *J*). Median and individual data points are shown. Fig 3, *A-D* and *F-J*, show pooled data from up to 11 experiments with wild-type 8-week-old mice (n = 3), *Dclre1c$^{leaky}$* 8-week-old mice (n = from 7 to 8), wild-type 8- to 10-month-old mice (n = from 3 to 14), and *Dclre1c$^{leaky}$* 8- to 10-month-old mice (n = from 8 to 27).

population stays stable in wild-type animals (Fig 4, *B* and *C*, and see Fig E3, *B* and *C*). Indeed, splenic absolute numbers of CD8$^+$ TCM cells increase 10-fold in old (median, 0.47 $\times$ 10$^6$) versus young (median, 0.04 $\times$ 10$^6$; $P<.001$) *Dclre1c$^{leaky}$* mice, although the overall number remains less than the wild-type cell number (median, 3.1 $\times$ 10$^6$ and 2.7 $\times$ 10$^6$ cells [not significant] in old and young mice, respectively).

The high T-cell activation in *Dclre1c$^{leaky}$* mice was also demonstrated by the increased percentage of cells expressing CD69 at their cell surfaces, a marker of early T-cell activation (Fig 4, *D*, and see Fig E3, *E*). By contrast, no difference in expression of CD127, KLRG1, or PD1 was observed in CD8$^+$ T-cell subsets (Fig 4, *E*); however, a transient boost in short-lived effector cells (SLECs) was observed in *leaky* mice at young ages, with resolution in older mice (see Fig E4 in this article's Online Repository at www.jacionline.org).

To determine whether the activated T cells in *leaky* mice were producing an inflammatory environment, we assessed cytokine release. Within *Dclre1c$^{leaky}$* mice, numbers of T$_H$1 (IFN-γ–secreting CD4$^+$ T cells), T$_H$2 (IL-4–secreting CD4$^+$ T cells), and T$_H$17 (IL-17–secreting CD4$^+$ T cells) cells were all increased compared with those in wild-type animals (Fig 4, *F*, and see Fig E3, *F*), with serum increases in IFN-γ levels also observed (Fig 4, *G*).

The inflammatory T-cell phenotype of *Dclre1c$^{leaky}$* mice was associated with immune pathology. More than 50% of *leaky* mice had a wasting disease with lower weight, poor grooming, an abnormal hunched posture, or signs of severe dermatitis (Fig 5, *A* and *B*, and see Fig E5, *A-C*, in this article's Online Repository at www.jacionline.org). When evaluated based on histology, all *leaky* analyzed mice showed signs of lymphoreticular infiltrates in different organs, including the lung, liver, gastrointestinal tract,

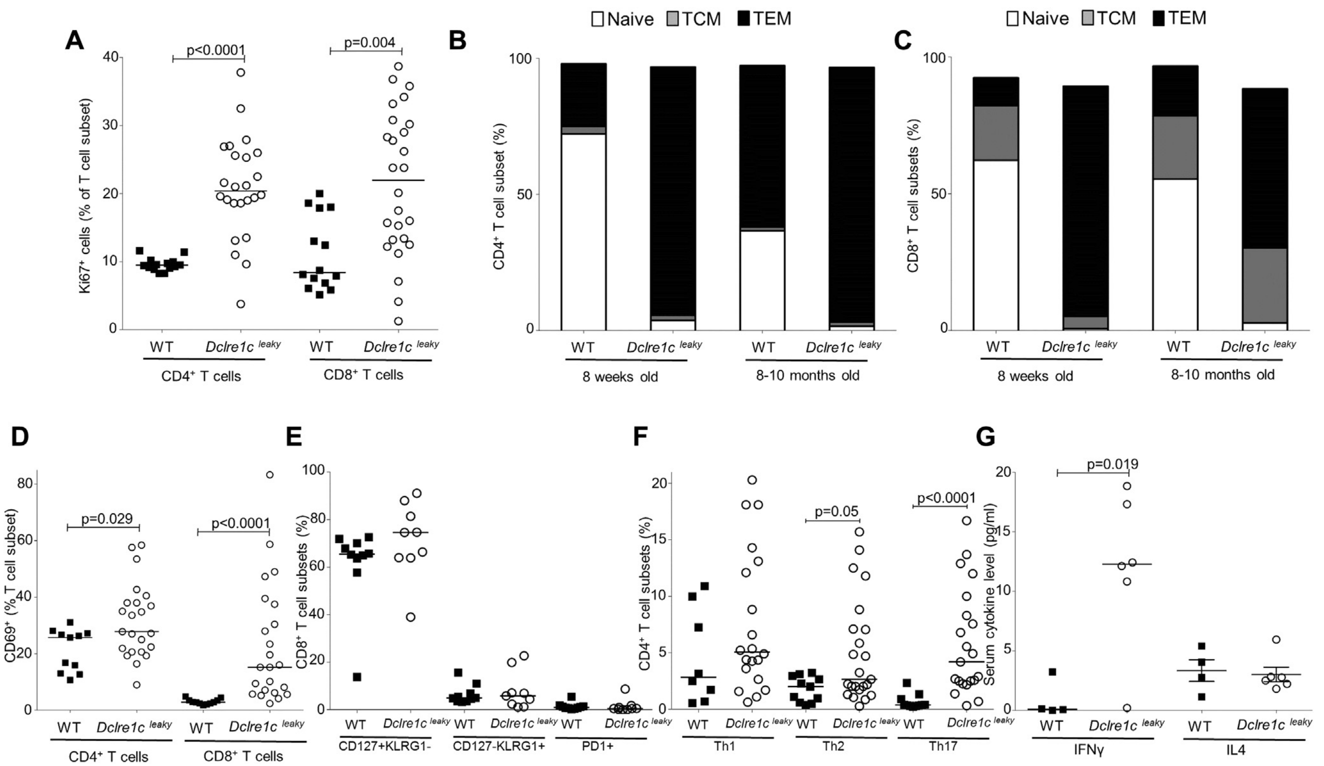


**FIG 4.** *Dclre1c$^{leaky}$* mice have increased T-cell activation and proinflammatory cytokine levels in serum. Splenic T cells from wild-type *(WT)* and *Dclre1c$^{leaky}$* mice were evaluated at 8 weeks and 8 to 10 months of age. T-cell subsets were analyzed by using flow cytometry. **A,** Percentage of $CD4^+$ and $CD8^+$ T cells expressing Ki67. **B** and **C,** T cells were characterized as $CD62L^+CD44^-$ naive cells, $CD62L^+CD44^+$ TCM cells, and $CD62L^-CD44^+$ effector memory T cells *(TEM)* for $CD4^+$ (Fig 4, *B*) and $CD8^+$ subsets (Fig 4, *C*). **D,** Percentage of $CD4^+$ and $CD8^+$ T cells expressing CD69. **E,** Percentage of $CD8^+$ T cells expressing CD127, KLRG1, and PD1. **F,** Splenocytes were stimulated *in vitro* for 4 hours with phorbol 12-myristate 13-acetate/ionomycin, and $CD4^+$ T cells were evaluated for cytokine secretion, including IFN-γ, IL-4, and IL-17. **G,** Serum levels of IFN-γ and IL-4. Median and individual data points are shown. Pooled data from up to 11 experiments are shown: wild-type 8-week-old mice (n = 3), *Dclre1c$^{leaky}$* 8-week-old mice (n = 8), wild-type 8- to 10-month-old mice (n = from 4 to 14), and *Dclre1c$^{leaky}$* 8- to 10-month-old mice (n = from 6 to 27).

pancreas, lymph nodes, and skin, with signs of severe vasculitis (Fig 5, *C*). Disease was accompanied by a high number of eosinophils in both the spleen and peripheral blood (Fig 5, *D*), and a substantial increase in IgE levels (>50,000 ng/mL) was detected in the sera of 26% of *leaky* mice (compared with 7% of age-matched control mice). Consistently, IL-5 in the sera of *Dclre1c$^{leaky}$* mice was detected at a higher level (see Fig E6 in this article's Online Repository at www.jacionline.org). In addition, tumors of a lymphoid origin developed in 15% of *Dclre1c$^{leaky}$* mice at 8 to 10 months of age (Fig 5, *A* and *E*, and see Fig E5, *D*), a level similar to that of spontaneous tumors reported in patients with *DCLRE1C* mutation and an LS phenotype.[3,4] The combined effect was an increased premature mortality rate in ARTEMIS mutant mice (18% at 8 months of age compared with 0% in wild-type siblings at the same age). This immune pathology places the *Dclre1c$^{leaky}$* mouse strain on the spectrum of clinical immune pathology observed in patients with LS or OS and *DCLRE1C* mutations.

## CTLA4-Ig treatment prevents immune pathology in ARTEMIS mutant mice with LS

The development of a new animal model that recapitulated the key clinical features of LS allowed the testing of potential therapeutic interventions. The *Dclre1c$^{leaky}$* phenotype was associated with peripheral T-cell activation, including high IL-4, high IgE, and increased eosinophil levels, which are characteristics of Treg cell deficiency and $T_H2$-mediated disease. These observations prompted us to treat *leaky* mice with CTLA4-Ig to investigate whether disease could be prevented by this treatment, which was shown previously to be effective in suppressing $T_H2$ responses in mice with low Treg cell numbers.[14] *Dclre1c$^{leaky}$* and littermate control mice (including heterozygous mice) were left untreated or received 25 mg/kg CTLA4-Ig every second week from the age of 8 weeks. Untreated *leaky* mice showed normal weight curves until 6 months of age, at which point wasting (Fig 6, *A*) and premature mortality (27% of mice) were noted (Fig 6, *B*). By contrast, the CTLA4-Ig–treated *leaky* mice did not exhibit wasting, and no premature mortality was observed (Fig 6, *A* and *B*). Furthermore, none of the *Dclre1c$^{leaky}$* mice receiving CTLA4-Ig treatment had any symptoms of skin inflammation (Fig 6, *C*, and see Fig E7 in this article's Online Repository at www.jacionline.org) or hyper-IgE (Fig 6, *D*). These observations indicate the efficacy of CTLA4-Ig for the autoimmune-related manifestations of LS. By contrast, however, colitis was not improved with CTLA4-Ig treatment, and 15% of *Dclre1c$^{leaky}$* mice treated with CTLA4-Ig had tumors, an incidence similar to the untreated

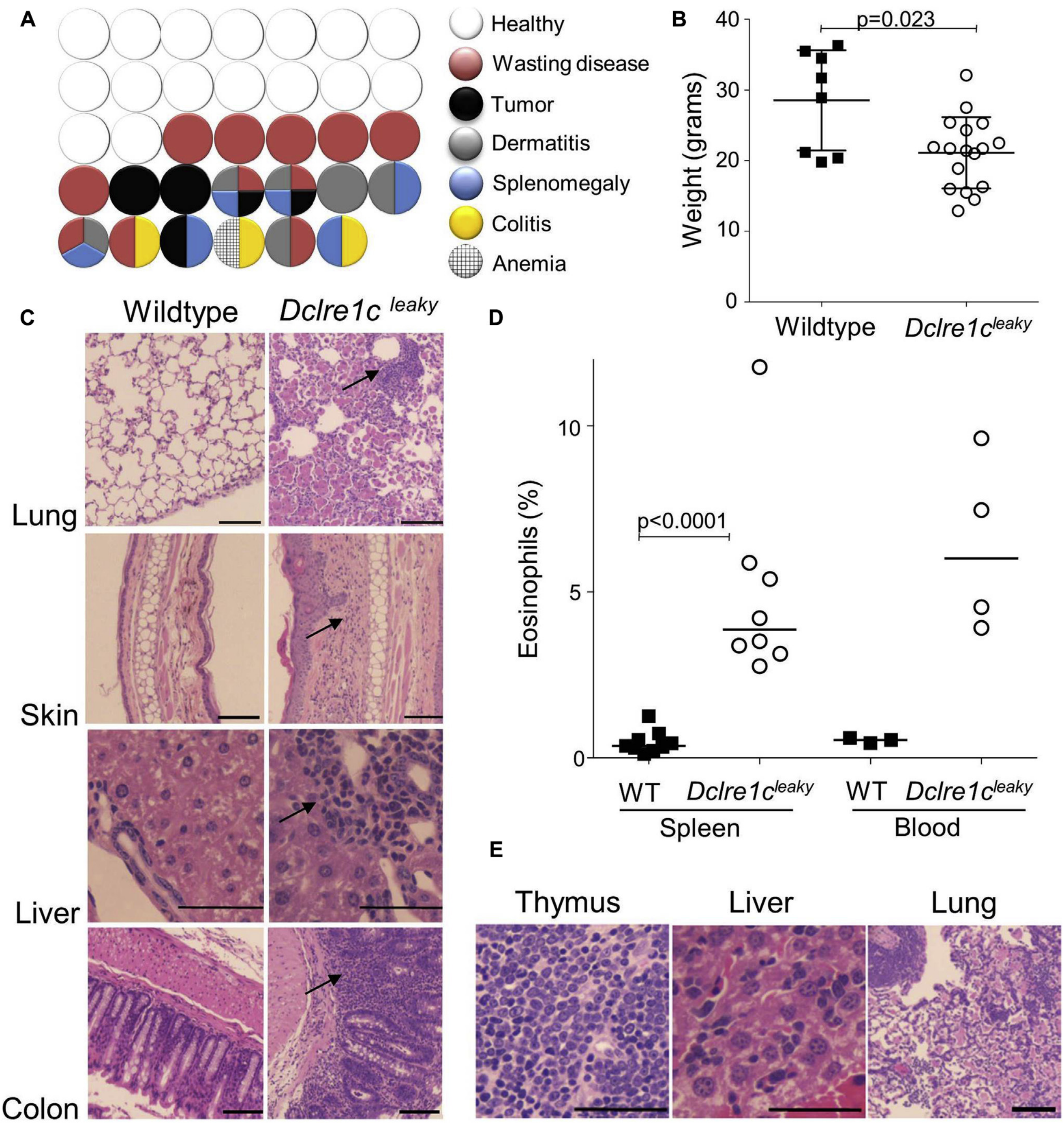


**FIG 5.** *Dclre1c*$^{leaky}$ mice are affected by inflammatory diseases and lymphoma. Mice were evaluated at 8 to 10 months of age for disease incidence and markers of inflammation. **A,** Thirty-four *leaky* mice were evaluated for pathological symptoms, and each *circle* represents an individual mouse. **B,** Mouse weight. **C,** Histology of lung, liver, skin, and colon of both wild-type *(WT)* and *Dclre1c*$^{leaky}$ mice. *Arrows* show lymphoreticular infiltrates. **D,** Percentage of eosinophils into the spleen and blood. **E,** Representative histology of a lymphocytic lymphoma from the thymus, infiltrating the liver and lung. Fig 5, *A*, shows pooled data from up to 11 experiments. Fig 5, *B*, shows pooled data from 5 experiments, wild-type mice (n = 8), and *Dclre1c*$^{leaky}$ mice (n = 17). Fig 5, *C* and *E*, show a representative histologic image. *Scale bars* = 50 μm. Fig 5, *D*, represents 1 experiment: wild-type mice (n = from 3 to 9) and *Dclre1c*$^{leaky}$ mice (n = from 4 to 7).

group, indicating that CTLA4-Ig administration does not prevent the development of thymic lymphoma (Fig 6, *C*).

Although the precise mechanism of action of CTLA4 is still under debate, there is strong evidence suggesting that reducing ligand access to the costimulation molecule CD28 constitutes one of its principal functions.[15] An immunologic analysis of the effects of CTLA4-Ig treatment on control and *leaky* mice found that the main immune phenotype caused by CTLA4-Ig treatment

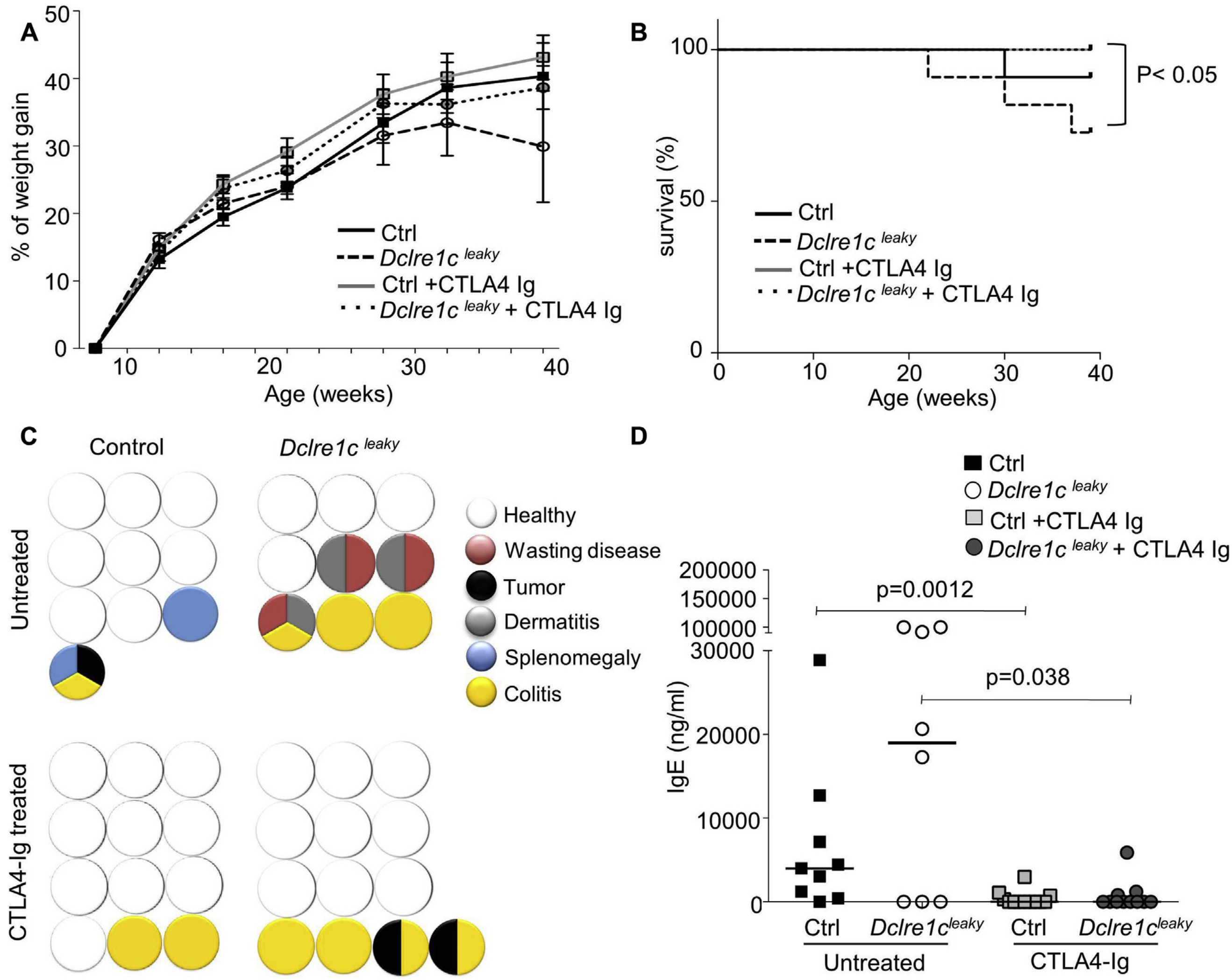


**FIG 6.** CTLA4-Ig treatment prevents immune pathology in *Dclre1c^leaky^* mice. *Dclre1c^leaky^* mice and littermate controls *(Ctrl)* were followed up for a longitudinal study with and without CTLA4-Ig treatment (25 mg/kg every 2 weeks starting at 8 weeks). Mice were evaluated at 40 weeks of age. **A,** Weight curve. **B,** Survival curve. **C,** Adverse events/pathological observations were monitored in all mice at the time of death, and each *circle* represents an individual mouse. **D,** IgE concentration in serum. Means and SEMs are shown for Fig 6, *A*, and medians and individual data points are shown for Fig 6, *D*. At the start of the study (Fig 6, *A* and *B*), untreated control mice (n = 11) and untreated *Dclre1c^leaky^* mice (n = 11), CTLA4-Ig–treated control mice (n = 12), and CTLA4-Ig–treated *Dclre1c^leaky^* mice (n = 13) were used. At the time of analysis (Fig 6, *C* and *D*), untreated control mice (n = 10), untreated *Dclre1c^leaky^* mice (n = 9), CTLA4-Ig–treated control mice (n = 12), and CTLA4-Ig–treated *Dclre1c^leaky^* mice (n = 13) were used.

was a pronounced and sustained decrease in $CD4^+$ T-cell counts, including a further reduction of the Treg cell subset (Fig 7, *A-C*, and see Fig E8, *A* and *B*, in this article's Online Repository at www.jacionline.org). This is in accordance with the fact that CD28 costimulation is critical for T-cell peripheral survival,[16] with a more profound requirement present in Treg cells.[17,18] Furthermore, we observed a lower percentage of $CD4^+$ T-cell proliferation (Fig 7, *D*, and see Fig E8, *C*) and activation (Fig 7, *E*, and see Fig E8, *D*) in the spleen and lymph nodes after CTLA4-Ig treatment. Regarding cytokine secretion, there was a strong reduction in the absolute number of cytokine-secreting T cells because of the generic blockade on T-cell activation (Fig 7, *F-H*), specifically in $T_H2$ cells as a reflection of better control of $T_H2$ over $T_H1$ by CTLA4-Ig.[14] In addition, levels of IFN-γ and TNF-α were significantly lower in the serum of *Dclre1c^leaky^* mice receiving CTLA4-Ig (Fig 7, *I* and *J*). Finally, it is worth noting that all significant immune differences induced by CTLA4-Ig treatment were observed in both littermate control and *Dclre1c^leaky^* mice, indicating that the successful ablation of immune pathology in *leaky* mice is driven by the same immunologic processes initiated by CTLA4 in control mice.

## DISCUSSION

Although complete T-cell deficiency presents as profound immunodeficiency, incomplete forms, prototypically OS and LS, manifest as a paradoxical copresentation of immunodeficiency and immune dysregulation with spontaneous inflammatory/

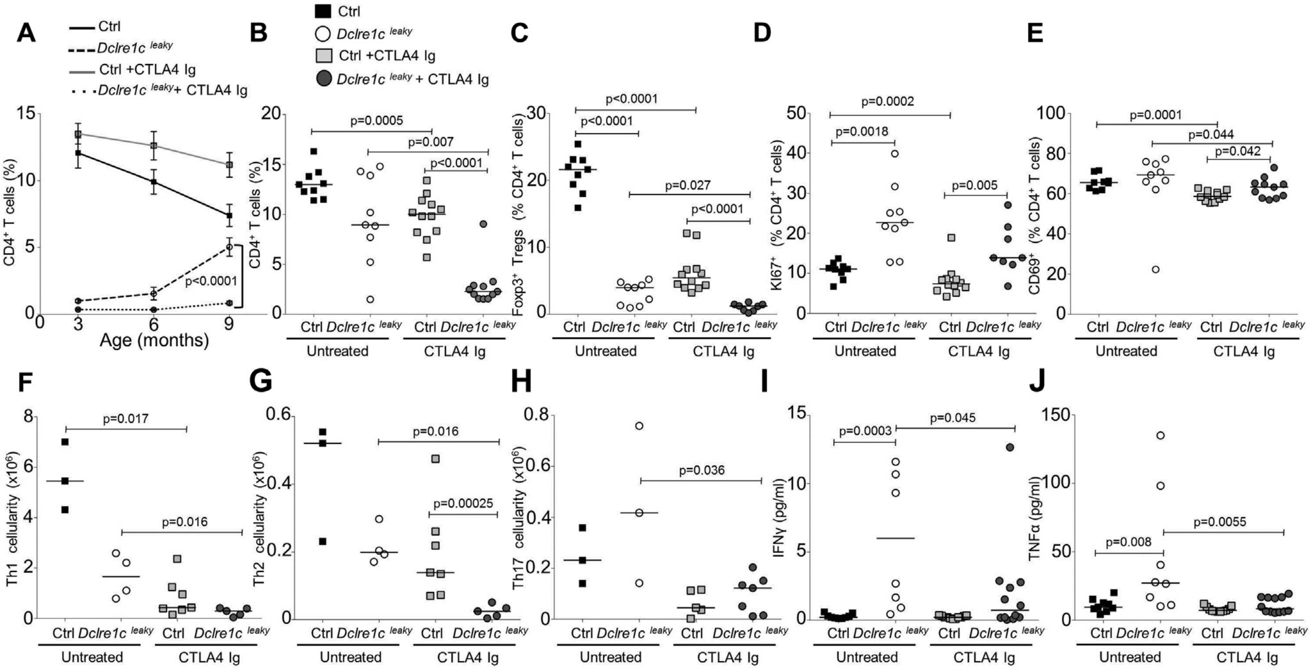


**FIG 7.** CTLA4-Ig treatment effectively decreases inflammation in *Dclre1c*$^{leaky}$ mice. *Dclre1c*$^{leaky}$ mice and littermate controls *(Ctrl)* received CTLA4-Ig (25 mg/kg) every 2 weeks starting at 8 weeks of age. Mice were evaluated at 40 weeks of age for the immune cell compartment in the spleen. **A,** Kinetics of CD4$^+$ T cells in blood at 3, 6, and 9 months of age. **B,** Percentage of total CD4$^+$ T cells. **C,** Percentage of Treg (CD4$^+$Foxp3$^+$ cells) within CD4$^+$ T cells. **D** and **E,** Ki67$^+$ cells (Fig 7, *D*) and CD69$^+$ cells (Fig 7, *E*). **F-H,** Absolute number of $T_H1$ (IFN-γ–secreting CD4$^+$ T cells Fig 7, *F*), $T_H2$ (IL-4–secreting CD4$^+$ T cells; Fig 7, *G*), and $T_H17$ cells (IL-17–secreting CD4$^+$ T cells; Fig 7, *H*). **I** and **J,** Serum level of IFN-γ (one very high value for *Dclre1c*$^{leaky}$ is not shown; Fig 7, *I*) and TNF-α (Fig 7, *J*). Medians and individual data points are shown. Fig 7, *A*, *I*, and *J*, represent 1 experiment, and Fig 7, *B-H*, represent data of 2 experiments. Untreated control mice (n = from 3 to 9) and untreated *Dclre1c*$^{leaky}$ mice (n = from 3 to 9), CTLA4-Ig–treated control mice (n = from 5 to 12) and CTLA4-Ig–treated *Dclre1c*$^{leaky}$ mice (n = from 5 to 11) were used.

autoimmune symptoms. Numerous hypotheses have been put forward to explain this paradox at the immunologic level, including a mismatch between available effector and Treg cell clones after oligoclonal expansion, reduced efficiency of thymic tolerance processes in the abnormal thymic tissue present, or a hyperstimulatory phenotype of dendritic cells created by peripheral T-cell deficiency.[6,19] However, a limited range of preclinical models has hampered the ability to test these models and develop therapeutic strategies.

Mutations in ARTEMIS drive clinical phenotypes that fall in the SCID-OS-LS spectrum. Mouse models, by contrast, show a much more restricted phenotypic range because of the concentration on "knockout" mutations. Standard ARTEMIS knockout mice possess a SCID-like phenotype, although the presence of T cells in the periphery suggests a partial redundancy of ARTEMIS for TCR rearrangement in mice.[8] Mutations in the C-terminal domain of ARTEMIS, which are more likely to promote a leaky phenotype in patients,[4] have only a partial block in B- and T-cell development[10]; however, none of these models present with clinical symptoms analogous to those experienced by patients with LS. In the ARTEMIS mouse model reported here, point mutation L219P results in a clinical phenotype that is very similar to that of patients with LS/OS, with inflammatory disorders in multiple organs. Specifically, *Dclre1c*$^{leaky}$ mice recapitulate key features of patients with LS/OS, including dermatitis, wasting disease, splenomegaly, inflammatory cytokines, high IgE levels, and hypereosinophilia. With symptomatic development in older mice, leaky mice fit within the LS clinical range, although with similarities to OS. Although no mutation in the 219 position has been described in a patient with SCID, a mutation in the nearby residue 228 within the same conserved region has been reported in a patient with a SCID phenotype and partial VDJ recombination and DNA repair activity *in vitro*.[4]

The serendipitous development of an LS preclinical model allowed for dissection of potential tolerance breakpoints and thus testing of intervention strategies. The most striking observation was the low number of Treg cells found in both the thymus and periphery. One could speculate that the only allowed V(D)J rearrangement in patients with LS is detrimental to Treg cell formation, maintenance, or both because of selection of TCR with a specific affinity.[20] This low Treg cell phenotype can account for the inflammatory $T_H1$/$T_H2$ profile observed in *Dclre1c*$^{leaky}$ mice because of the asymmetry in Treg cell control over the 2 immune arms.[14] Additional homeostatic "space filling" pressures can be extrapolated from the oligoclonal expansion and adoption of the effector memory T-cell phenotype observed in T cells. The logical extension of this immunologic presentation is that therapeutic intervention requires substitution for Treg cell deficiency, enhanced suppression of the $T_H2$ response, and a counteraction of the enhanced CD80/CD86 stimulatory profile of lymphopenic dendritic cells.

Current treatment for inflammatory manifestation in patients with LS/OS is based on nonspecific immunosuppressive drugs, such as corticosteroids and cyclosporine.[13,21] Although these treatments show some limited success, the combination of limited efficacy and undesirable side effects leave room for clinical improvement. New therapeutic approaches are being directed toward better targeted and specific treatment with less side effects, as illustrated with the use of thrombopoietin receptor agonist in the case of thrombocytopenia.[21] The immunology-directed rationale of changes identified in our preclinical model identified CTLA4-Ig, a soluble version of CTLA4, as a key therapeutic candidate.

CTLA4-Ig meets all of the intervention criteria listed above. First, as a potent suppressive molecule used by Treg cells for immune suppression,[22] CTLA4-Ig can be substitutive for Treg cells. Second, CTLA4-Ig is highly effective at quenching $T_H2$ responses.[14] Third, CTLA4-Ig effectively competes with CD80/CD86 for CD28 binding,[15] countering the increased expression of these molecules in lymphopenic dendritic cells. Because bimonthly administration of CTLA4-Ig to *Dclre1c*$^{leaky}$ mice resolved inflammation, prevented tissue damage, and improved overall survival, the immunologic rationale of CTLA4-Ig selection for murine LS treatment can be regarded as validated. Although abatacept demonstrates high efficiency in rodent studies, when considering clinical translation, additional options become available, with belatacept demonstrating higher affinity toward human CD86.[23]

Overall, our study identified a novel mutation of ARTEMIS, resulting in a murine preclinical model of LS. Consistent with $CD4^+$ T cells being the driver of inflammatory disease in patients with LS[24] and based on assessment of the immunologic disturbances observed, CTLA4-Ig proved an effective drug to prevent disease manifestation and increase survival. By contrast, no improvement was observed in the increased incidence of lymphoma in these mice, which mirrors the patient's presentation,[4] indicating a mechanistically independent origin for the oncological components of disease. In addition, colitis seems to be resistant to CTLA4-Ig treatment. This observation is in accordance with clinical trials that showed failure of CTLA4-Ig in the treatment of patients with Crohn disease or ulcerative colitis[25] secondary to the resistance of inhibition of $T_H17$ by CTLA4.[21] Together, these results call for a carefully controlled trial of CTLA4-Ig treatment of patients with OS/LS to investigate the potential for treating the autoimmune/inflammatory components of disease.

**Key messages**

- **The *Dclre1c*$^{leaky}$ mouse recapitulates the symptoms and immunologic features of patients with LS/OS.**
- **CTLA4-Ig efficiently controls inflammation in these mice through tight regulation of $CD4^+$ T cells.**

## REFERENCES

1. Le Deist F, Poinsignon C, Moshous D, Fischer A, de Villartay J-P. Artemis sheds new light on V(D)J recombination. Immunol Rev 2004;200:142-55.
2. Shearer WT, Dunn E, Notarangelo LD, Dvorak CC, Puck JM, Logan BR, et al. Establishing diagnostic criteria for severe combined immunodeficiency disease (SCID), leaky SCID, and Omenn syndrome: the Primary Immune Deficiency Treatment Consortium experience. J Allergy Clin Immunol 2014;133:1092-8.
3. Moshous D, Pannetier C, Chasseval Rd Rd, Deist Fl Fl, Cavazzana-Calvo M, Romana S, et al. Partial T and B lymphocyte immunodeficiency and predisposition to lymphoma in patients with hypomorphic mutations in Artemis. J Clin Invest 2003;111:381-7.
4. Felgentreff K, Lee YN, Frugoni F, Du L, van der Burg M, Giliani S, et al. Functional analysis of naturally occurring DCLRE1C mutations and correlation with the clinical phenotype of ARTEMIS deficiency. J Allergy Clin Immunol 2015;136:140-50.e7.
5. Ege M, Ma Y, Manfras B, Kalwak K, Lu H, Lieber MR, et al. Omenn syndrome due to ARTEMIS mutations. Blood 2005;105:4179-86.
6. Liston A, Enders A, Siggs OM. Unravelling the association of partial T-cell immunodeficiency and immune dysregulation. Nat Rev Immunol 2008;8:545-58.
7. Fontenot JD, Rasmussen JP, Williams LM, Dooley JL, Farr AG, Rudensky AY. Regulatory T cell lineage specification by the forkhead transcription factor foxp3. Immunity 2005;22:329-41.
8. Rooney S, Sekiguchi J, Zhu C, Cheng HL, Manis J, Whitlow S, et al. Leaky Scid phenotype associated with defective V(D)J coding end processing in artemis-deficient mice. Mol Cell 2002;10:1379-90.
9. Barthels C, Puchałka J, Racek T, Klein C, Brocker T. Novel spontaneous deletion of artemis exons 10 and 11 in mice leads to T- and B-cell deficiency. PLoS One 2013;8:e74838.
10. Huang Y, Giblin W, Kubec M, Westfield G, St Charles J, Chadde L, et al. Impact of a hypomorphic Artemis disease allele on lymphocyte development, DNA end processing, and genome stability. J Exp Med 2009;206:893-908.
11. Li L, Salido E, Zhou Y, Yannone SM, Dunn E, Feeney AJ, et al. Targeted disruption of the Artemis murine counterpart results in SICD and defective V(D)J recombination that is partially corrected with bone marrow transplantation. J Immunol 2005;174:2420-8.
12. Jacobs C, Huang Y, Masud T, Lu W, Westfield G, Giblin W, et al. A hypomorphic Artemis human disease allele causes aberrant chromosomal rearrangements and tumorigenesis. Hum Mol Genet 2011;20:806-19.
13. Villa A, Notarangelo LD, Roifman CM. Omenn syndrome: inflammation in leaky severe combined immunodeficiency. J Allergy Clin Immunol 2008;122:1082-6.
14. Tian L, Altin JA, Makaroff LE, Franckaert D, Cook MC, Goodnow CC, et al. Foxp3+ regulatory T cells exert asymmetric control over murine helper responses by inducing Th2 cell apoptosis. Blood 2011;118:1845-53.
15. Walker LSK, Sansom DM. Confusing signals: recent progress in CTLA-4 biology. Trends Immunol 2015;36:63-70.
16. Shi Y, Radvanyi LG, Sharma A, Shaw P, Green DR, Miller RG, et al. CD28-mediated signaling in vivo prevents activation-induced apoptosis in the thymus and alters peripheral lymphocyte homeostasis. J Immunol 1995;155:1829-37.
17. Tang Q, Henriksen KJ, Boden EK, Tooley AJ, Ye J, Subudhi SK, et al. Cutting edge: CD28 controls peripheral homeostasis of CD4+CD25+ regulatory T cells. J Immunol 2003;171:3348-52.
18. Franckaert D, Dooley J, Roos E, Floess S, Huehn J, Luche H, et al. Promiscuous Foxp3-cre activity reveals a differential requirement for CD28 in $Foxp3^+$ and $Foxp3^-$ T cells. Immunol Cell Biol 2015;93:417-23.
19. Milner JD, Fasth A, Etzioni A. Autoimmunity in severe combined immunodeficiency (SCID): lessons from patients and experimental models. J Clin Immunol 2008;28(suppl 1):S29-33.
20. Hsieh C-S, Lee H-M, Lio C-WJ. Selection of regulatory T cells in the thymus. Nat Rev Immunol 2012;12:157.
21. Seidel MG. Autoimmune and other cytopenias in primary immunodeficiencies: pathomechanisms, novel differential diagnoses, and treatment. Blood 2014;124:2337-45.
22. Wing K, Onishi Y, Prieto-Martin P, Yamaguchi T, Miyara M, Fehervari Z, et al. CTLA-4 control over Foxp3+ regulatory T cell function. Science 2008;322:271-5.
23. Ford ML, Adams AB, Pearson TC. Targeting co-stimulatory pathways: transplantation and autoimmunity. Nat Rev Nephrol 2014;10:14-24.
24. Khiong K, Murakami M, Kitabayashi C, Ueda N, Sawa S, Sakamoto A, et al. Homeostatically proliferating CD4 T cells are involved in the pathogenesis of an Omenn syndrome murine model. J Clin Invest 2007;117:1270-81.
25. Sandborn WJ, Colombel J, Sands BE, Rutgeerts P, Targan SR, Panaccione R, et al. Abatacept for Crohn's disease and ulcerative colitis. Gastroenterology 2012;143:62-9.e4.

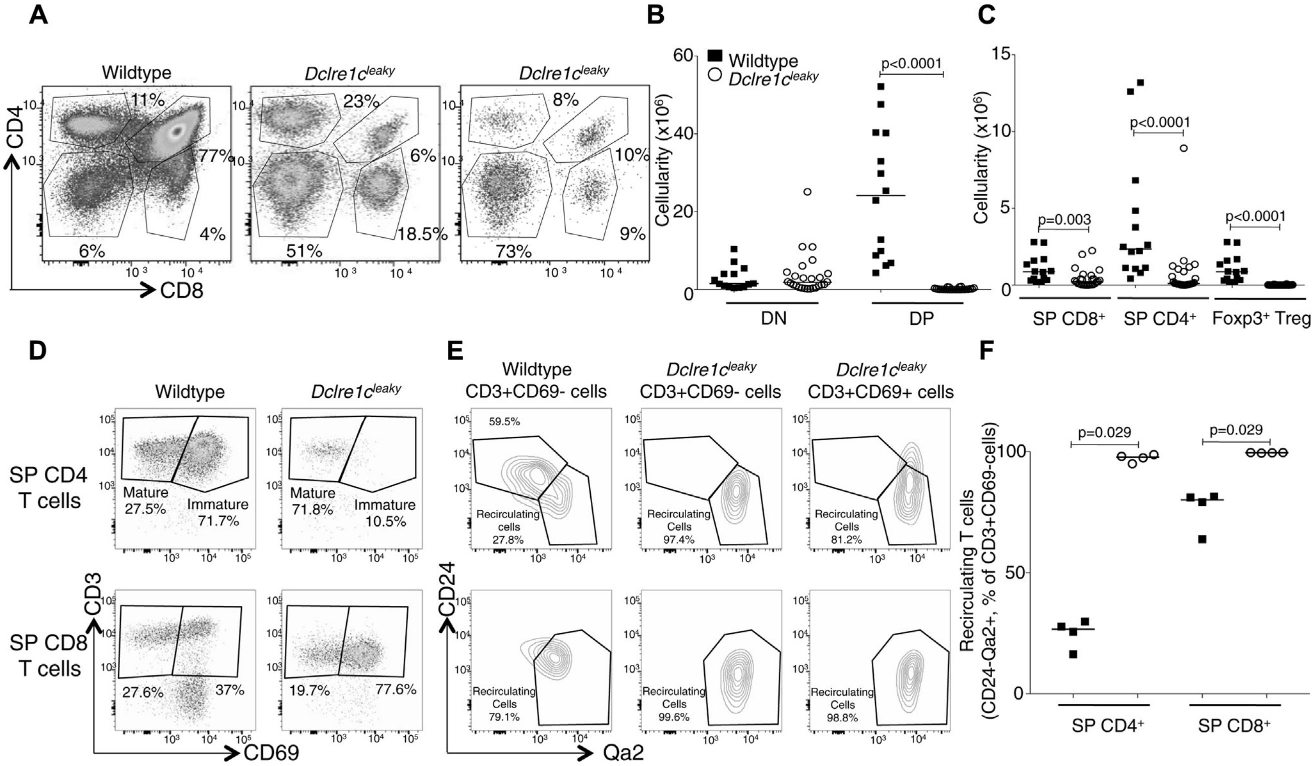


**FIG E1.** T-cell developmental defects in $Dclre1c^{leaky}$ mice. Thymi from 8- to 10-month-old wild-type and $Dclre1c^{leaky}$ mice (Fig E1, *A-C*) or 10-week-old mice (Fig E1, *D-F*) were analyzed for cell numbers and T-cell subsets by using flow cytometry. **A,** Representative flow cytometric plot from the thymus, including 2 mice within the $Dclre1c^{leaky}$ phenotype spectrum. **B** and **C,** Thymocyte subset absolute cell numbers for double-negative *(DN)* and double-positive (*DP*; Fig E1, *B*) and the $CD4^+$ and $CD8^+$ single-positive *(SP)* and Treg cell (Fig E1, *C*) subsets. **D,** Representative flow cytometric plot for mature ($CD3^+CD69^-$) and immature ($CD3^+CD69^+$) cells within $CD4^+$ and $CD8^+$ SP subsets. **E,** Representative flow cytometric plot for the presence of recirculating cells ($CD24^-Qa2^+$) within $CD3^+CD69^-$ or $CD3^+CD69^+$ cells in $CD4^+$ and $CD8^+$ SP subsets. **F,** Percentage of recirculating T cells in the mature $CD3^+CD69^-$ subsets of the $CD4^+$ and $CD8^+$ SP compartment. Median and individual data points are shown. Fig E1, *B* and *C*, Pooled data from up to 11 experiments were used: wild-type mice (n = 14) and $Dclre1c^{leaky}$ mice (n = from 24 to 26). Fig E1, *D-F*, represents a single experiment: wild-type mice (n = 4) and $Dclre1c^{leaky}$ mice (n = 4).

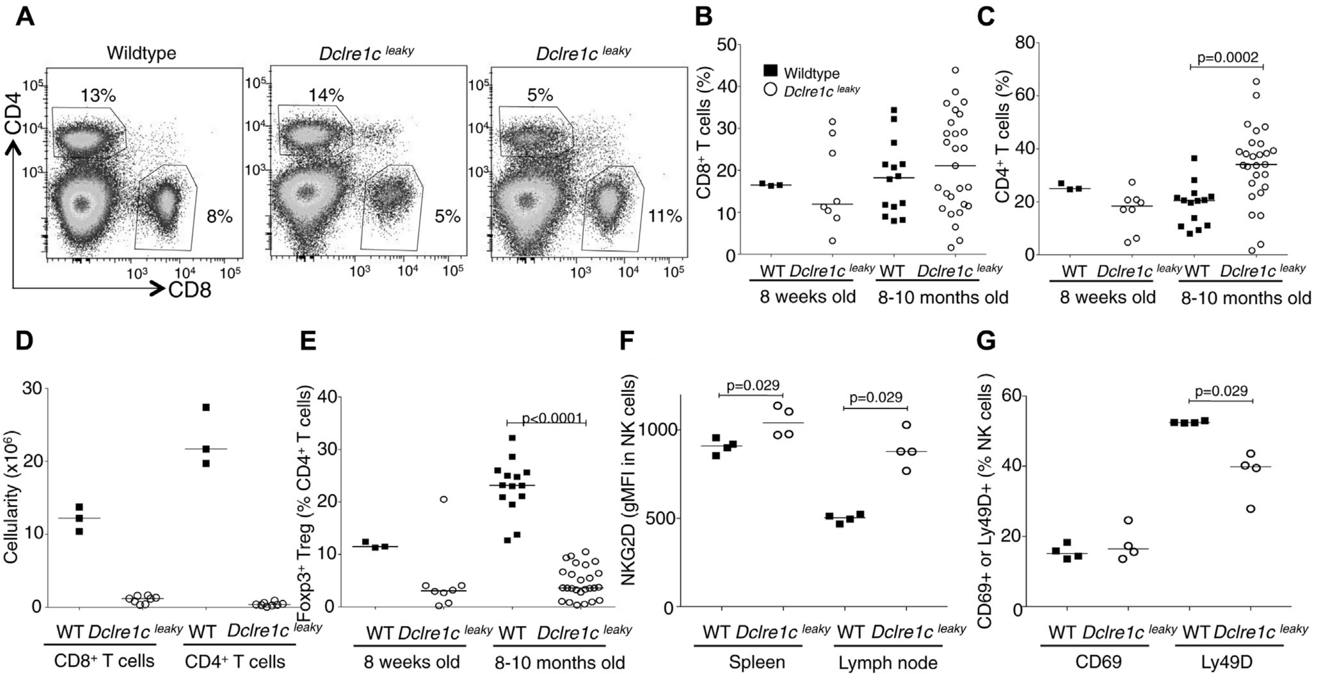


**FIG E2.** *Dclre1c^leaky* mice have an LS phenotype in the periphery. Lymph nodes from wild-type *(WT)* and *Dclre1c^leaky* mice were evaluated at 8 weeks of age and between 8 and 10 months of age. T-cell subsets were analyzed by using flow cytometry *(A-E)*. **A,** Representative flow cytometric plot from the lymph nodes, including 2 mice within the *Dclre1c^leaky* phenotype spectrum. **B** and **C,** Percentage of total $CD8^+$ (Fig E2, *B*) and $CD4^+$ (Fig E2, *C*) T cells. **D,** Absolute numbers of $CD8^+$ and $CD4^+$ T cells in the spleen at 8 weeks of age. **E,** Percentage of Treg cells ($CD4^+Foxp3^+$ cells) in the lymph nodes. **F,** NKG2D geometric mean fluorescence expression *(gMFI)* in splenic natural killer cells in 10-week-old mice. **G,** CD69 and Ly49D percentages in splenic natural killer cells in 10-week-old mice. Median and individual data points are shown. Fig E2, *B-E*, Pooled data from up to 11 experiments are shown: wild-type 8-week-old mice (n = 3), *Dclre1c^leaky* 8-week-old mice (n = 8), wild-type 8- to 10-month-old mice (n = 14), and *Dclre1c^leaky* 8- to 10-month-old mice (n = from 26 to 27). Fig E2, *F* and *G*, represent a single experiment: wild-type mice (n = 4) and *Dclre1c^leaky* mice (n = 4).

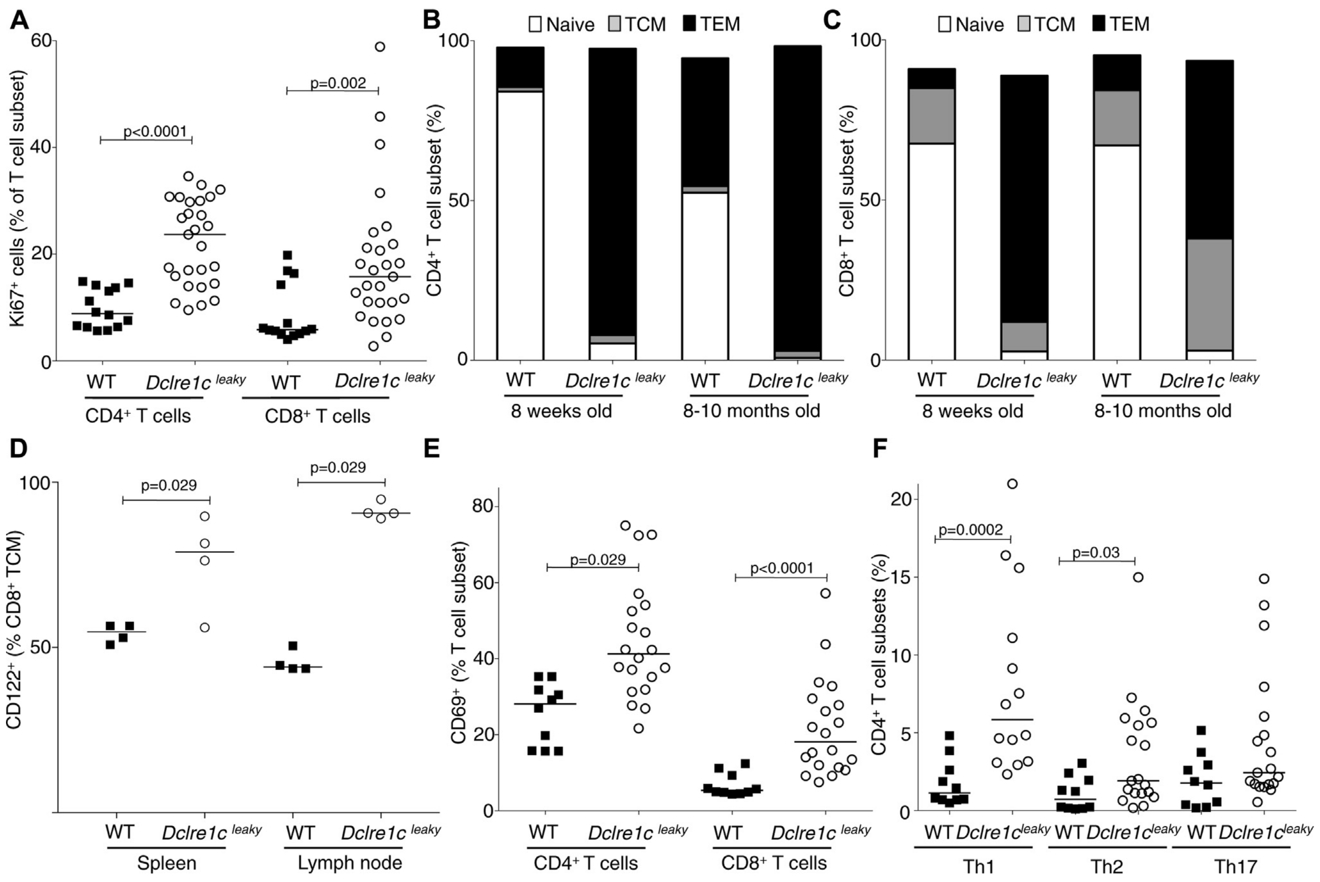


**FIG E3.** *Dclre1c^leaky^* have increased T-cell activation and proinflammatory cytokines in serum. Lymph nodes from wild-type *(WT)* and *Dclre1c^leaky^* mice were evaluated at 8 weeks of age and between 8 and 10 months of age (Fig E3, *A-C*, *E*, and *F*). T-cell subsets were analyzed by using flow cytometry. **A,** Percentage of $CD4^+$ and $CD8^+$ T cells expressing Ki67. **B** and **C,** $CD4^+$ and $CD8^+$ T-cell subpopulations were characterized as $CD62L^+CD44^-$ naive cells, $CD62L^+CD44^+$ TCM cells, and $CD62L^-CD44^+$ effector memory T cells *(TEM)* by using flow cytometry. Fig E3, *B*, shows the percentage of $CD4^+$ naive, TCM, and TEM cells. Fig E3, *C*, Percentage of $CD8^+$ naive, TCM, and TEM cells. **D,** Percentage of $CD122^+$ cells within the $CD8^+$ TCM cell subsets in 10-week-old mice. **E,** Percentage of $CD4^+$ and $CD8^+$ T cells expressing CD69. **F,** Cells from lymph nodes were stimulated *in vitro* for 4 hours with phorbol 12-myristate 13-acetate/ionomycin and $CD4^+$ T cells evaluated for cytokine secretion, including IFN-$\gamma$, IL-4, and IL-17. Median and individual data points are shown. Fig E3, *A-C*, *E*, and *F*, show pooled data from up to 11 experiments: wild-type 8-week-old mice (n = 3), *Dclre1c^leaky^* 8-week-old mice (n = 8), wild-type 8- to 10-month-old mice (n = 14), and *Dclre1c^leaky^* 8- to 10-month-old mice (n = from 26 to 27). Fig E3, *D*, represents a single experiment: wild-type mice (n = 4) and *Dclre1c^leaky^* mice (n = 4).

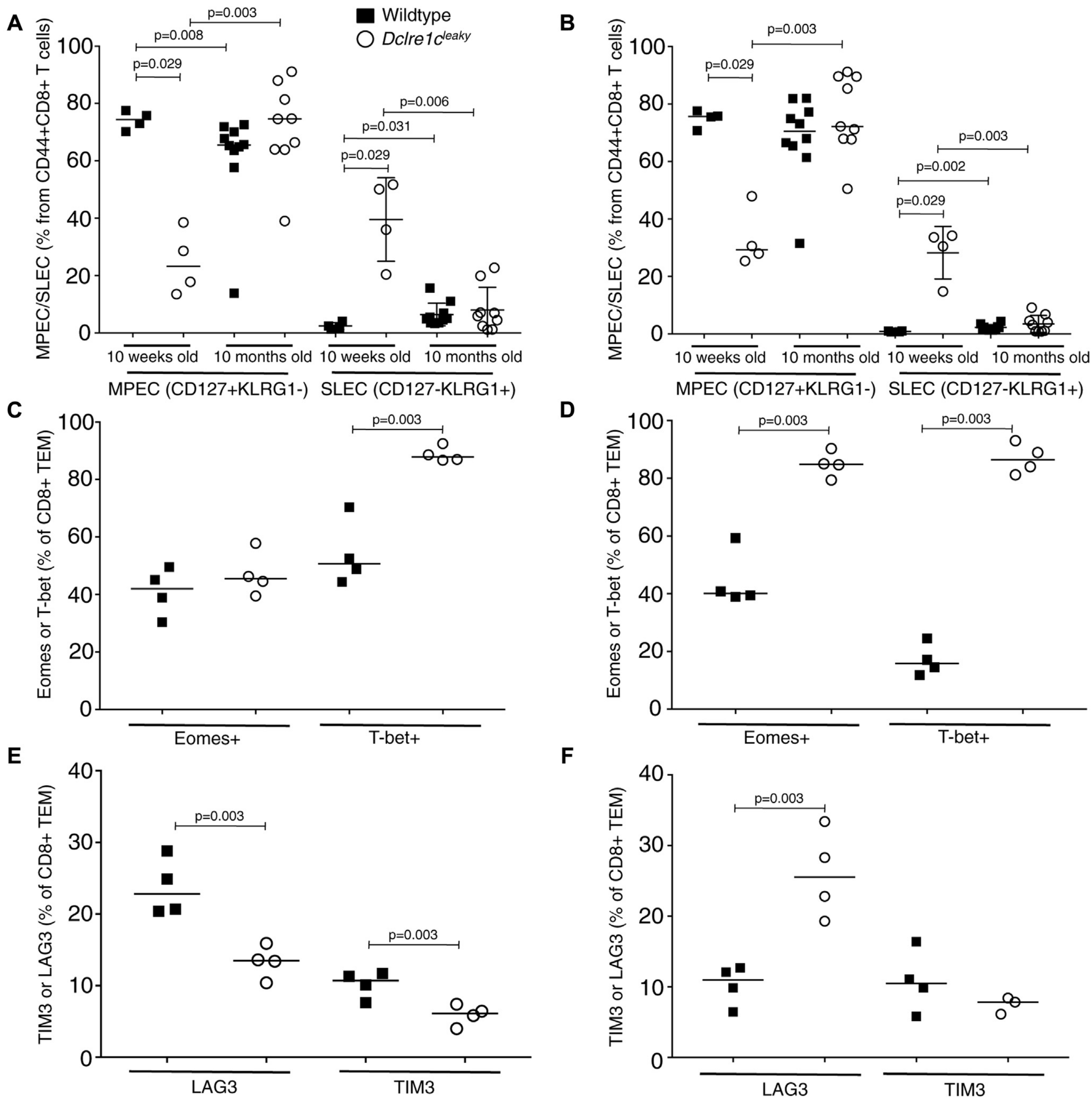


**FIG E4.** Increased short-lived effector cell counts in young *Dclre1c^leaky* mice. $CD8^+$ T cells were analyzed in a cohort of 10-week-old mice by using flow cytometry in the spleen and lymph nodes and compared with values in older mice (8-10 months old). **A** and **B,** Percentage of $CD127^+KLRG1^-$ memory precursor effector cells *(MPEC)* and $CD127^-KLRG1^+$ short-lived effector cells *(SLEC)* within $CD44^+CD8^+$ subsets in the spleen (Fig E4, *A*) and lymph nodes (Fig E4, *B*). **C** and **D,** Percentage of $Eomes^+$ and $T\text{-}bet^+$ cells within $CD8^+CD44^+CD62L^-$ subsets and effector memory T cells *(TEM)* in the spleen (Fig E4, *C*) and lymph nodes (Fig E4, *D*) of 10-week-old mice. **E** and **F,** Percentage of $LAG3^+$ and $TIM3^+$ cells within $CD8^+CD44^+CD62L^-$ subsets and effector memory T cells *(TEM)* in the spleen (Fig E4, *E*) and lymph nodes (Fig E4, *F*) of 10-week-old mice. Median and individual data points are shown. Fig E4, *A-F*, represent a single experiment: wild-type mice (n = 4) and *Dclre1c^leaky* mice (n = 4).

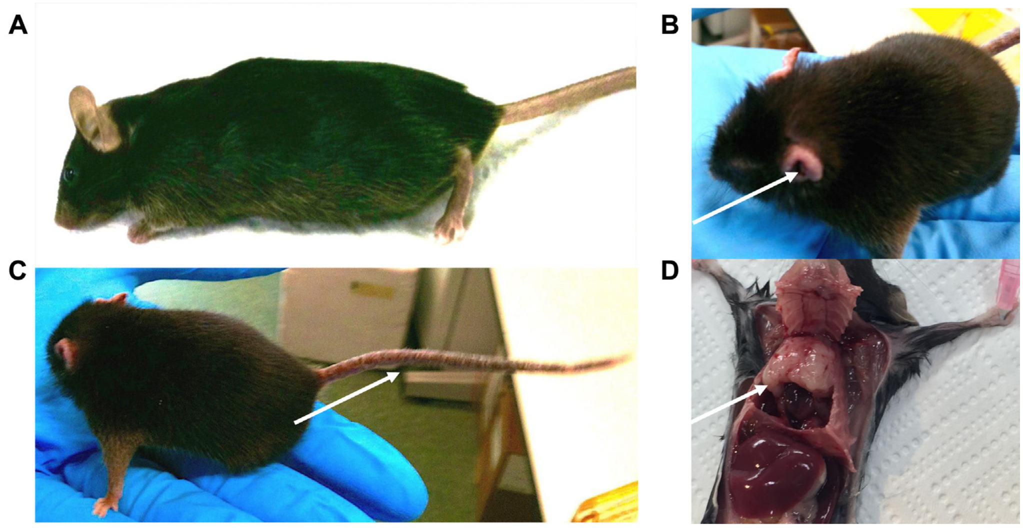


**FIG E5.** *Dclre1c*$^{leaky}$ mice are affected by inflammatory diseases and are at higher risk for lymphoma. Mice from 8 to 10 months of age were evaluated at the time of death for disease incidence. **A,** Representative picture of a wild-type mouse. **B** and **C,** Representative picture of a *Dclre1c*$^{leaky}$ mouse, including hunched posture and dermatitis of the ear (*arrow*; Fig E5, *B*) and tail (*arrow*; Fig E5, *C*). **D,** Representative picture of a *Dclre1c*$^{leaky}$ mouse with a thymic tumor *(arrow)*.

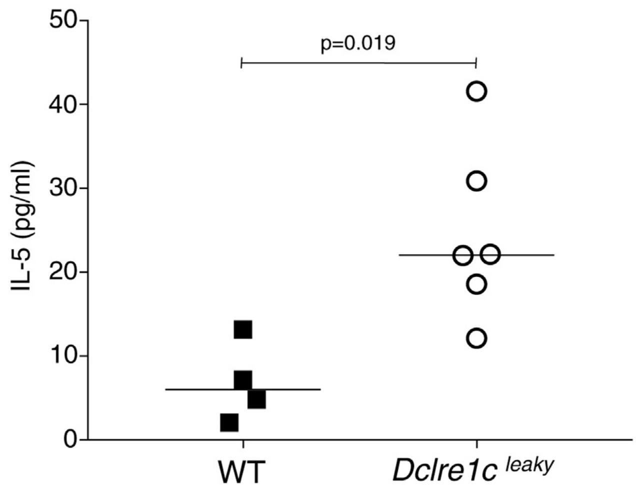


**FIG E6.** IL-5 levels are increased in sera of *Dclre1c*$^{leaky}$ mice. Sera from mice from 8 to 10 months of age were evaluated for the presence of IL-5 by using the MSD assay. Median and individual data points are shown. Pooled data are from 2 experiments: wild-type (n = 4) and *Dclre1c*$^{leaky}$ (n = 6) mice.

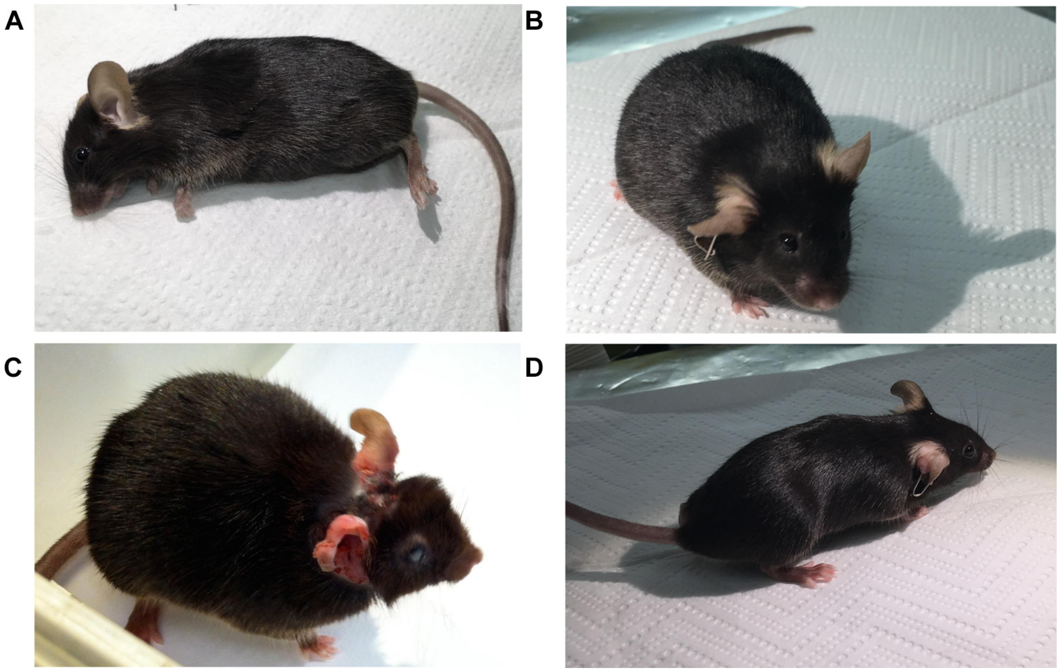


**FIG E7.** CTLA4-Ig treatment prevents immune pathology in *Dclre1c*$^{leaky}$ mice. *Dclre1c*$^{leaky}$ mice and littermate controls *(Ctrl)* were followed up for a longitudinal study with or without CTLA4-Ig treatment (25 mg/kg) every 2 weeks starting at 8 weeks of age. Mice were evaluated at 40 weeks of age. Representative pictures are of an untreated control mouse **(A)**, a control mouse after CTLA4-Ig treatment **(B)**, an untreated *Dclre1c*$^{leaky}$ mouse **(C)**, and a *Dclre1c*$^{leaky}$ mouse after CTLA4-Ig treatment **(D)**.

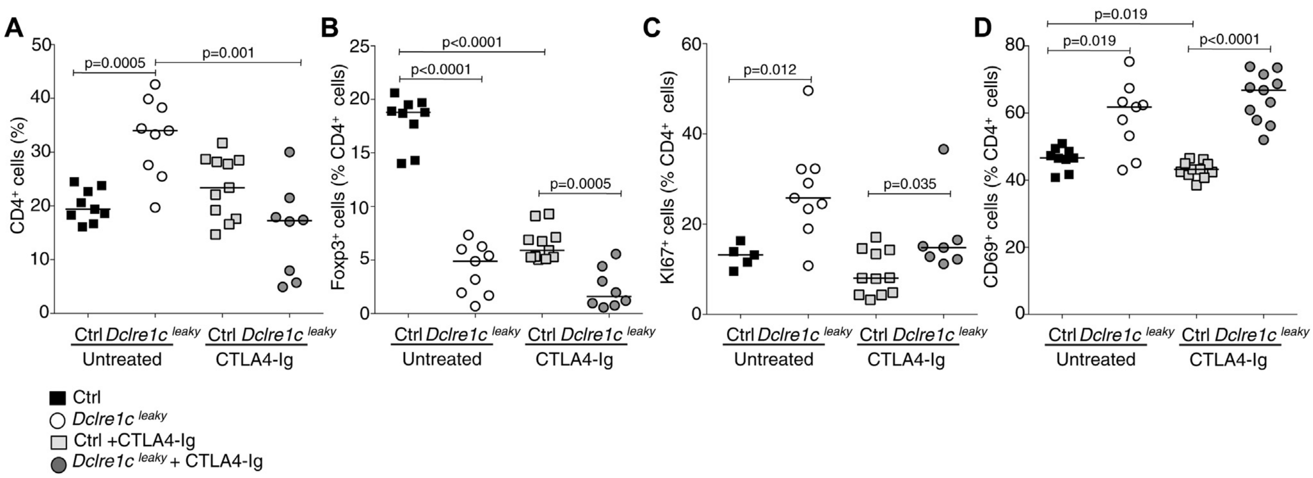


**FIG E8.** CTLA4-Ig treatment decreased total CD4$^+$ T-cell counts in *Dclre1c$^{leaky}$* mice and the overall inflammatory cytokine environment. *Dclre1c$^{leaky}$* mice and littermate controls *(Ctrl)* received CTLA4-Ig (25 mg/kg) every 2 weeks starting at 8 weeks of age. Mice were evaluated at 40 weeks of age for the immune cell compartment in lymph nodes. **A,** Percentages of total CD4$^+$ T cells. **B,** Percentage of Treg cells from total CD4$^+$ T cells. **C** and **D,** Ki67$^+$ cells (Fig E8, *C*) and CD69$^+$ cells (Fig E8, *D*) from total CD4$^+$ T cells. Median and individual data points are shown. Representative data are of 2 experiments: untreated control mice (n = from 5 to 10), untreated *Dclre1c$^{leaky}$* mice (n = 9), CTLA4-Ig−treated control mice (n = 11), and CTLA4-Ig−treated *Dclre1c$^{leaky}$* mice (n = from 7 to 11).